CHINESE JOURNAL OF PHYSICS VOL. 52, NO. 1-II February 2014

Review

Ionic Valence Change of Metal Ions in Solution by Femtosecond Laser Excitation Accompanied by White-Light Laser

Nobuaki Nakashima,[1,2,*] Ken-ichi Yamanaka,[3] Ayaka Itoh,[2] and Tomoyuki Yatsuhashi[2]

[1] *Toyota Physical and Chemical Research Institute, Nagakute, Aichi 480-1192, Japan; Institute for Laser Technology, Osaka, 550-0004, Japan*
[2] *Department of Chemistry, Graduate School of Science, Osaka City University, Sumiyoshi, Osaka 558-8585, Japan*
[3] *Toyota Central R&D Labs., Inc., Nagakute, Aichi 480-1192, Japan*

(Received August 30, 2013)

Three lanthanide ions (Ln^{3+}), Ln = Eu, Sm, and Yb, and two transition metals, Fe^{3+} and Ag^{+}, were found to be reduced to the corresponding Ln^{2+}, Fe^{2+}, and Ag_n in methanol or aqueous solution upon irradiation with intense femtosecond laser pulses. The major excitation wavelength was 800 nm and single-photon-non-resonant with the electronic transitions of metal ion solutions. Laser pulses with wavelengths of 970, 1190, and 1930 nm were used for particular cases. Whenever the white-light laser was generated, the reductions were observed. The reduction mechanisms would be explained in terms of self-focusing, solvated electron formation followed by trapping the electron. The electron ejection under focused beam conditions in solution has been known to be accompanied by white-light laser. In the exceptional case of Fe^{3+} at 800 nm, two-photon excitation of the charge transfer state followed by the reduction would be operative. Fe^{2+} was detected even with an intensity lower than the threshold of the white-light laser generation.

DOI: 10.6122/CJP.52.504 PACS numbers: 82.50.Bc, 82.50.Pt

I. INTRODUCTION

Femtosecond filamentation, particularly with respect to phenomena in air and its applications, have been extensively studied and reviewed [1]. Many interesting applications have emerged, including rain making [2] and generation of mid-infrared pulses [3]. In this paper we introduce a chemical application in solution induced by femtosecond laser filamentation. Two of the authors found Eu^{2+} ion formation accompanied by white laser generation in Eu^{3+} ions in methanol [4] and subsequently found an $Sm^{3+} \rightarrow Sm^{2+}$ reaction [5]. The excitation wavelength of 800 nm was non-resonant with the electronic transitions of the 3+ metal ions. The reactions would be induced by electron ejection by femtosecond filamentation accompanied by white laser generation. We have suggested that these reactions are similar to those in radiation chemistry in solution [4]. In this context, it is worth pointing out two recent papers in relation to femtosecond filament chemistry. One of these studies

*Electronic address: nakashima@toyotariken.jp

found that carbon nano-particles form on the benzene/water interface under the generation of femtosecond laser plasma [6]. In the other paper, femtosecond filamentation was applied to cancer therapy, yielding ultra-high dose rates without any dose deposit in front or behind the target volume [7]. This paper will show that the metal ion reduction by femtosecond laser excitation is a general phenomenon by extending the reduction to a few metal ion systems. The metal ion reaction is a simple redox reaction; therefore, this study will provide fundamental characteristics of the chemical reactions induced by femtosecond filamentation in solution and in tissues.

We have added another lanthanide ion, Yb^{3+}, and two transition metal ions, Fe^{3+} and Ag^{+}. Reduced ions for all of the above systems have been distinctly observed with absorption, emission, and/or visual color changes under femtosecond laser irradiation. The reactions of Eu^{3+} in solution have a similarity with Eu^{2+} formation in optical glasses from Eu^{3+} by infrared femtosecond laser pulses. It has been suggested that an electron is ejected and that Eu^{3+} ions act as electron-trapping centers [8, 9]. The reactions between electrons and Eu^{3+} ions induced by femtosecond pulses are similar to those in radiation chemistry in solutions. Irradiation of γ-rays can produce an electron that will subsequently reduce Eu^{3+} to Eu^{2+} [10, 11]. The rate constants between the metal ions, including molecules, and electrons have been studied in detail and accumulated for more than 1500 examples in radiation chemistry [12, 13].

In this paper, we will try to clarify the following points.

i) To generalize metal ion reactions by femtosecond laser pulses, we adopt Yb^{3+} solution as the third example of lanthanide ions. The reaction of the Yb^{3+} system should be similar to those of the other two lanthanide ions, $Eu^{3+}$and Sm^{3+}. These three ions have small oxidation potentials and fast rate constants with a solvated electron in common [12–14].

ii) We will try to extend the reduction to two transition metal ions: Fe^{3+} and Ag^{+}.

iii) Multiphoton absorption absorption followed by reduction would be included, because the inorganic systems have a charge transfer (CT) absorption band in the UV-Vis ranges. Redox reactions can be induced by the CT band excitation. The three lanthanide Eu, Sm, and Yb ions have photochemically active CT bands which are active for single as well as two-photon excitation [5, 15–18]. We have examined the reactions with femtosecond pulses with different wavelengths. The oxalate Fe^{3+} complex is used as one of the transition metal ion systems. The complex has been used for chemical actinometry [19, 20]and its photochemical mechanism has been extensively studied [21–24]. The CT band below 400 nm is known to be two-photon active for a 694.3-nm laser [25]. We will see that the oxalate Fe^{3+} complex is two-photon active for 800-nm femtosecond pulses in this paper. Pulses with a long wavelength of 1190 nm are used to suppress the two-photon chemistry, but multiphoton absorption could still occur. For organic molecules, multiphoton absorption of 5–7 photons occurs just below the intensity white-light laser generation [26, 27].

iv) The reductions are similar to the reactions in radiation chemistry, because the electron ejection is the primary step in both excitation methods. Many metal ion reductions including the ions treating here have been accumulated in the field of radiation chemistry [12–14]. In the present study we will consider an Ag^{+} system, because Ag^{+} re-

duction and Ag_n^+ cluster and/or nanoparticle formation have been studied by γ-radiolysis [28 a]. It will be of interest to see whether similar reactions actually occur by femtosecond pulse excitation. It should be noted that Ag nanoparticle formation has been reported with femtosecond laser irradiation under high laser intensities, where solvent break down occurs [28 b]. We observed Ag nanoparticles under weak laser intensities, where white-light laser emission was barely visible. The reactions under the break down conditions should be compared with plasma induced reactions, while the present results would have some similarities with γ-radiolysis.

II. EXPERIMENTAL

For Yb^{3+} experiments, a linearly polarized femtosecond laser pulse with a central wavelength of 800 nm was used [29]. It was delivered from a Ti:sapphire laser system Alpha 100/XS, Thales Laser, at a repetition rate of 100 Hz. The transform-limited pulse had a duration of 43 fs. The pulse width was measured with a single-shot autocorrelator (Thales, TAIGA), and the total pulse energy was measured with a power meter (Gentec eo, PS-310B). Infrared pulses at central wavelengths of 970 and 1930 nm were converted from an 800-nm fundamental pulse using an optical parametric oscillator and amplifier (Quantronix, TOPAS). The spectral widths were about 40 nm for the 970-nm pulse and 80 nm for the 1930-nm one. The infrared pulses from the parametric converter were selected by reflecting it with several dielectric mirrors. The pulse width was estimated to be 130 fs. This value was obtained at 1.4 μm by a second order scanning autocorrelator (APE, PulseCheck). The cell contained 0.16 cm^3 Yb^{3+} solution in a 2 (width) $\times$ 4 (depth) $\times$ 20 (height) mm^3 quartz cell. Samples were degassed to avoid a back reaction due to air oxidation of Yb^{2+}. The femtosecond laser beam was introduced in the direction of 0.4 cm depth, and absorption of Yb^{2+} was measured with a path length of 0.4 cm.

For Fe^{3+} and Ag^+ experiments, 800-nm and 1190-nm pulses were used. The output of a mode-locked Ti:sapphire oscillator (Coherent, Vitesse), which was pumped by the second harmonic generation (SHG) of a continuous wave Nd^{3+}:YVO_4 laser (Coherent, Verdi), was amplified with a regenerative amplifier (Coherent, Legend), which was pumped by a Nd^{3+}:YLF laser (Coherent, Evolution) [30]. The output of the amplifier (2.4 W, 100 fs fwhm, 1 kHz, 800 nm) was converted to 1190-nm pulses with a spectral width of 30 nm using an optical parametric amplifier (OPA) system (Coherent, OPerA). The averaged power of the laser pulse and the pulse energy were monitored with power meters (Gentec TPM310) with photo-diode (THORLABS PDA50B) combinations. The cell contained 0.3 cm^3 0.1–0.2 M of Fe^{3+} solution in a 5 (width) $\times$ 10 (depth) mm^2 quartz cell for 1190-nm pulses and in a plastic cell for 800-nm pulses.

A plano-convex lens with a focal length of 200 mm was used to focus the laser beam into a sample cell located 20 mm before the focal point for the Eu^{3+} system only [4], and at the focal point for other all systems. The product Yb^{2+} was detected by its absorption spectrum with a peak at 367 nm [17]. The Yb^{3+} complexes and its photochemistry have been described previously [17]. A solution of Fe^{3+} potassium ferrioxalate was prepared and the

formed Fe^{2+}ion was detected by the standard chemical actinometry method [20]. Briefly, after irradiation, the Fe^{2+} ion is complexed with 1,10-phenanthroline, which has a broad absorption spectrum peak at 510 nm with a molar extinction coefficient of 1.1×10^4 $M^{-1}cm^{-1}$. In the present study, the Fe^{2+} complex concentration was measured at 520 nm with spectrophotometers with a Biochrom CO7500 Colourwave and a Shimadzu UV 3600. For the 1190-nm experiments, potassium tris(oxalate)ferrate(III) trihydrate ($K_3Fe_2(C_2O_4)_3 \cdot 3H_2O$) (Wako Chemicals) and D_2SO_4 were dissolved in D_2O in order to minimize the absorption of the excitation infrared pulse. Ag^+ ion aqueous solution was prepared according to the literature [28], but the Ag^+ concentration was 5×10^{-3} M with 0.01 M sodium polyacrylate, PANa (MW: 2100) and 0.13 M 2-propanol. The Fe^{3+} and Ag^+ samples were air saturated.

III. RESULTS

III-1. The third lanthanide ion reaction of $Yb^{3+} \rightarrow Yb^{2+}$ followed by $Eu^{3+} \rightarrow Eu^{2+}$ and $Sm^{3+} \rightarrow Sm^{2+}$ reactions

The energy levels of the three lanthanide ions and excitation wavelengths are shown in Fig. 1. The figure was constructed based on 4f electronic levels [14], the charge transfer (CT) states [31], and luminescence lifetimes [17, 32]. The ionic valence changes have been observed for Eu^{3+} and Sm^{3+} by femtosecond pulses with a wavelength of 800 nm [4, 5], and a Yb^{3+} ion system is further examined in this paper as the third active lanthanide ion by femtosecond pulses with 970 and 1930 nm in addition to 800 nm wavelengths. The major wavelength of 800 nm is non-resonant with the electronic levels for all cases, and the 970 and 1930-nm wavelengths are one photon and two photon resonances with an electronic level of Yb^{3+}. The CT states with the counter chloride ion are photo-reactive and locate in the UV region. If these levels are excited with a single photon and/or stepwise two-photon, each lanthanide system shows a reduction to Ln^{2+} [5, 15–18]. When we discuss the reduction of the lanthanide ions on irradiation with an intense laser pulse, we have to think about whether multiphoton excitation to the CT levels might be included or not.

Figure 2 shows the appearance of the Yb^{2+} spectra with a peak at 367 nm by irradiation with 1.8×10^5 shots of 800-nm wavelength. The spectral shape of Yb^{2+} is the same as that produced by UV irradiation [17]. The Yb^{2+} is formed with 970-nm 130-fs pulses with 1.8×10^5 shots in a pulse energy range of 3–40 μJ and at 1930 nm with a single pulse energy of 4–10 μJ. The femtosecond pulse with a central wavelength of 970 nm has a width of 40 nm; therefore, it can be a resonant wavelength with the $^2F_{7/2} \leftarrow {}^2F_{5/2}$ transition, and the 1930-nm pulse can be regarded as a two-photon resonant wavelength. The spectral width is 70 nm from 920 to 990 nm between the luminescent level of $^2F_{5/2}$ and the ground state of $^2F_{7/2}$. The central wavelength of the transition is 975 nm in CH_3OH with the molar extinction coefficient of 2.6 $M^{-1}cm^{-1}$. No other 4f electronic excited state exists below the charge transfer state, which is shorter than 280 nm.

The following two points are derived from the results in Figure 3. i) The thresholds for the appearance of Yb^{2+} were 2–4 μJ and there was no clear difference for the formation of Yb^{2+} between the excitation wavelengths of 800 and 970 nm. These results indicate

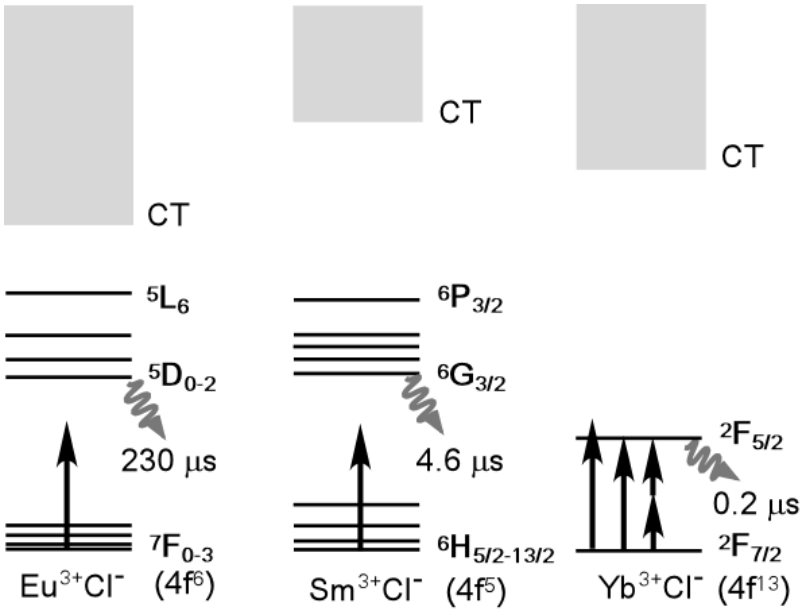

FIG. 1: Energy levels and excitation wavelengths of the lanthanide Ln^{3+} systems. The major excitation wavelength 800 nm is non-resonant with the electronic levels, as shown by the longest vertical arrows. For the Yb^{3+} system, 970 and 1930 nm are the resonant wavelengths. The photoreactive charge transfer (CT) levels are indicated with the gray areas in the UV region. The emission lifetimes in methanol are indicated.

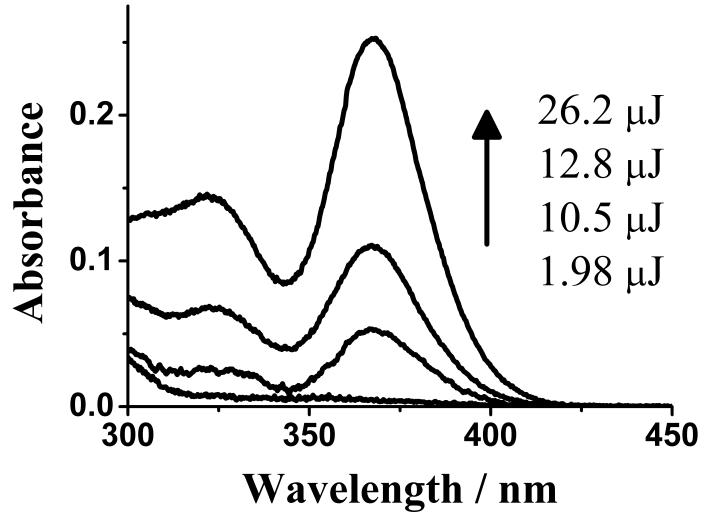

FIG. 2: Yb^{2+} absorption spectra appear around 367 nm by irradiating an Yb^{3+} system of 0.1 M of $YbCl_3 \cdot 6H_2O$ with 0.5 M of 15-crown-5-ether in methanol with 1.8×10^5 shots of 800-nm and 43-fs pulses. The pulse energies are indicated.

that the formation efficiencies for the two wavelengths were almost the same for the input energy. ii) The slopes were about 1.7 for 800-nm pulse and 1.8 for 970-nm pulse from the absorbance values of Yb^{2+} vs. laser intensity in the logarithmic scale.

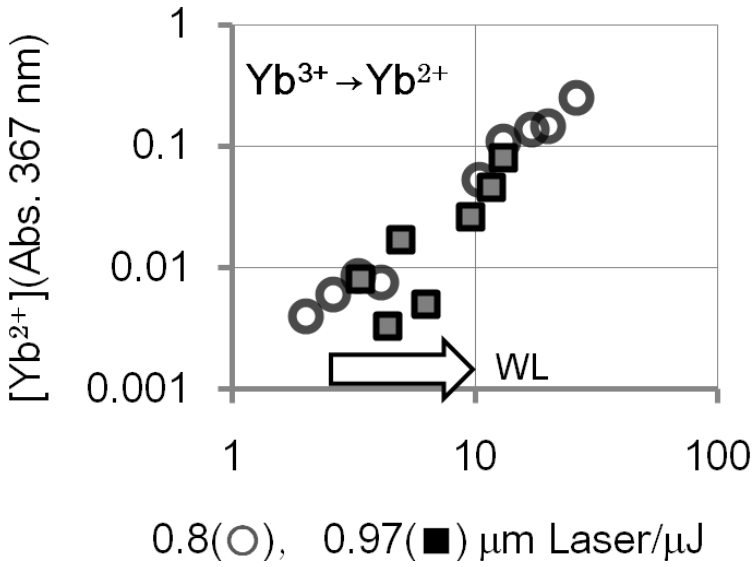

FIG. 3: (a) Yb^{2+} formation as absorbance at 367 nm for a 0.4 cm cell length after 1.8×10^5 shots of irradiation of 0.1 M of $YbCl_3 \cdot 6H_2O$ with 0.5 M of 15-crown-5-ether in methanol. ◯: At a wavelength of 800 nm with a duration of 43 fs; ■: at a wavelength of 970 nm with a duration of 130 fs. The arrow indicates the range where white-light laser was visually detectable with a pulse with a duration of 43 fs at 800 nm.

In order to reach the CT state (< 280 nm), three photons for 800-nm pulses are required; in addition, four photons for 970-nm pulses and more than seven photons for 1930-nm pulses are needed by multiphoton excitation. The conversion efficiency to Yb^{2+} should be drastically reduced by going from the 800-nm excitation to 970- and 1930-nm excitations, if the multiphoton mechanism worked (for an additional discussion see section IV-2). The present observations do not support the multiphoton excitation to the CT levels. The efficiencies were not largely different between 800- and 970-nm excitations. Even at the 1930-nm pulse, Yb^{2+} absorption was detectable at 4–10 μJ pulse excitation. The slopes of the formation of Yb^{2+} did not support the expected orders if the multiphoton processes were operative. The low order might be expected for the resonant wavelengths at 970 nm. The slope of 1.8 did not support the one-photon plus three-photon absorption mechanism.

The white-light laser was visually observed on a white paper 20 cm behind the sample cell and the threshold was also around 3 μJ for both the 800- and 970-nm wavelengths. The spectrum of the white-light laser was essentially the same as that reported elsewhere [33]. The spectra have a $1/e^2$ width of about 50 nm at 3–10 μJ of irradiation energy and spread over the entire visible range at 20 μJ of laser energy.

The thresholds for the formation of Yb^{2+} can be regarded as the same for the white laser generation. The generation of white-light laser is an indication of an electron injec-

tion [1, 33–35]. Immediately after the ejection the electron will be solvated to less than 1 ps to form e^-_{sol} as has been observed in the case of a solvent of water [36]. We conclude that the mechanism of Ln^{2+} formation is as follows, where the Ln = Eu, Sm, and Yb.

$$\begin{aligned} &CH_3OH \xrightarrow{nh\nu} CH_3OH^+ + e^-_{sol}, \\ &Ln^{3+} + e^-_{sol} \rightarrow Ln^{2+}, \end{aligned} \tag{1}$$

where e^-_{sol} is an solvated electron by methanol.

III-2. Fe^{3+} →Fe^2 as a first example of transition metal ions

The photo-redox reaction of the $Fe^{3+}(C_2O_4)^{3-}_3$ complex in aqueous solutions has been used for chemical actinometry. Parker et al. first suggested the use of the Fe^{3+} to Fe^{2+} photo-redox reaction as a sensitive chemical actinometer [19], and its quantum yields have been studied in detail and summarized in the 254–436 nm range [20]. The accepted overall reaction is presented by the following scheme [21–24]:

$$2[Fe^{3+}(C_2O_4)_3]^{3-} \xrightarrow{h\nu} 2[Fe^{2+}(C_2O_4)_2]^{2-} + 2CO_2 + C_2O^{2-}_4. \tag{2}$$

The reaction involves CT band excitation, dissociation to $CO_2\bullet^-$ radical/solvated electron (e^-_{sol}) ejection, and subsequent reactions of $CO_2\bullet^-$ radical and e^-_{sol} with the parent Fe^{3+} complex to reduce Fe^{3+} to Fe^{2+} by intermolecular electron transfer.

The absorption spectrum of the $Fe^{3+}(C_2O_4)^{3-}_3$ complex in acidic water has the CT band in the UV region with its shoulder at 280 nm with 5×10^3 $M^{-1}cm^{-1}$ as shown in Figure 4 [21]. The other band in the visible region, which is assigned to a d-d transition, is not clear in this figure because of its small coefficient of 1 $M^{-1}cm^{-1}$. The photoproducts Fe^{2+} can be detected by forming an *o*-phenanthroline complex [20], which has a reasonably broad, strong absorption with 1.1×10^4 $M^{-1}cm^{-1}$ at 510 nm, as shown in Figure 4.

The pictures in Figure 4 show the color change of $Fe^{3+}(C_2O_4)^{3-}_3$ solution induced by irradiating 800-nm femtosecond pulses. The solution color was yellow before irradiation due to weak absorption starting at 400 nm for the 0.1 M $K_3Fe^{3+}(C_2O_4)_3$ solution. After irradiation of pulses with an energy of 12 μJ/pulse and a duration of 100 fs, at 1 kHz for 5 min, followed by addition of *o*-phenanthrolin, the red color appeared with an absorbance of more than 1.0 even at 540 nm. The detailed results are shown in Figure 5 with an absorbance Fe^{2+} complex under an irradiation energy in the range of 0.2–12 μJ/pulse 0.25–30 min. The vertical scale represents concentrations of $Fe^{2+}(o\text{-phen})^{2-}_3$ and was normalized to absorbance at 520 nm for 1 cm cell length per 1 min. The dotted line has a slope of 2.0 for the log-log scale. A deviation from the line was seen before an energy of 10 μJ/pulse.

The dotted line has a slope of 2.0 for the log-log scale. Two-photon excitation to the CT state followed by reduction to Fe^{2+} would be the major reaction mechanism. In fact two-photon excitation to the CT state followed by reduction to Fe^{2+} has been reported by using a nanosecond ruby laser at 694.3 nm with a coefficient of 1.5×10^{-50} cm^4 s/photon [25]. The same mechanism would be operative at the present, long wavelength of 800 nm.

Figure 6 shows $Fe^{3+} \rightarrow Fe^{2+}$ conversion on irradiation with 1190-nm laser pulses. The absorbance of Fe^{2+} complex per at 520 nm one minute under an irradiation energy in

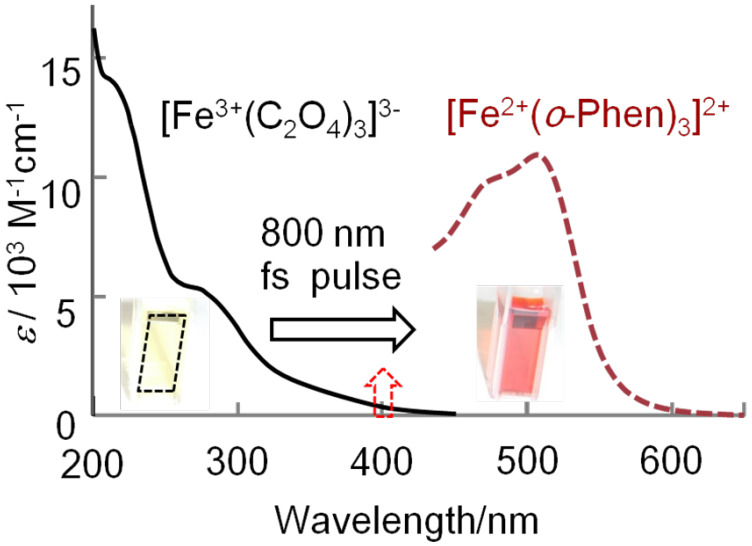

FIG. 4: The solid line is the absorption spectrum of $Fe^{3+}(C_2O_4)_3^{3-}$ in acidic water in the UV region with a light yellow color, and the broken line represents $Fe^{2+}(o\text{-phen})_3^{2-}$ in the Vis region. Femtosecond pulse irradiation of the 0.1 M $K_3Fe^{3+}(C_2O_4)_3$ solution turns the yellow color to red. The dotted rhomboid is a guide for the sample cell. The vertical arrow with a broken line is a wavelength of two-photon absorption of a pulse at 0.8 μm.

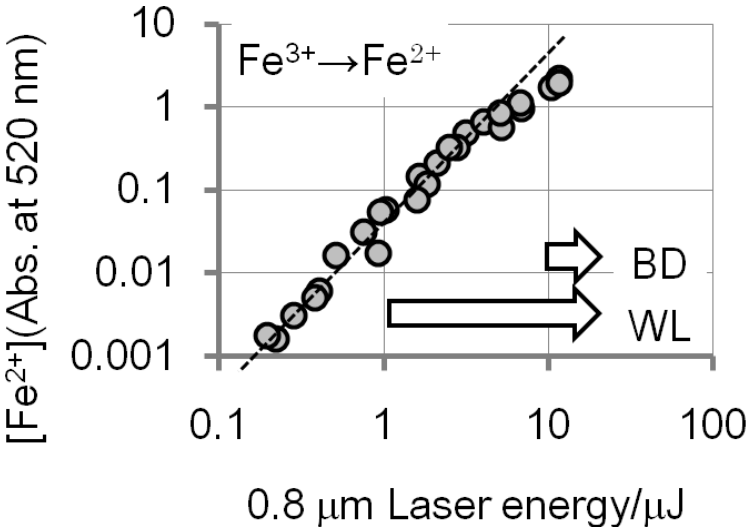

FIG. 5: $Fe^{3+} \rightarrow Fe^{2+}$ conversion on irradiation with 800-nm, 100-fs laser pulses of 0.1 M $K_3Fe^{3+}(C_2O_4)_3$ aqueous solution. The vertical scale represents log (absorbance) at 520 nm for 1 cm cell length per 1 min of $Fe^{2+} - o$-phenanthroline complex and the horizontal scale is log (laser energy in a unit of μJ/pulse). An arrow with WL is a region of energy where white-light laser was visually observed and an arrow with BD shows an energy region where bright spots were occasionally observed visually.

the range of 1.3–12 μJ/pulse for 5 – 751 min is shown. The smallest absorbance value in the figure was observed as 0.00 in absorbance at 1.45 μJ of laser energy after 751 min irradiation; therefore, the maximum value would be $0.005/751 = 6.7\times10^{-6}$ in absorbance per min. The reduction mechanism seems to be solvent ionization followed by the electron tarp reaction on the basis of two important differences from those for an excitation wavelength of 800 nm. i) A single straight line cannot fit most of the observed points, but a sharp drop is seen in an energy range lower than that where white-light laser is observable. A multiphoton excitation and reduction mechanism does not seem to support the present observation, though the three-photon energy corresponds to 397 nm and reaches the CT state. ii) A low conversion efficiency to Fe^{2+} from the input laser energy is observed and about 1/10 of that with an excitation wavelength of 800 nm at several micro Joule of laser energy. But it would not be low enough to explain them by the mechanism based on the three-photon absorption (for a detailed discussion see section IV-2).

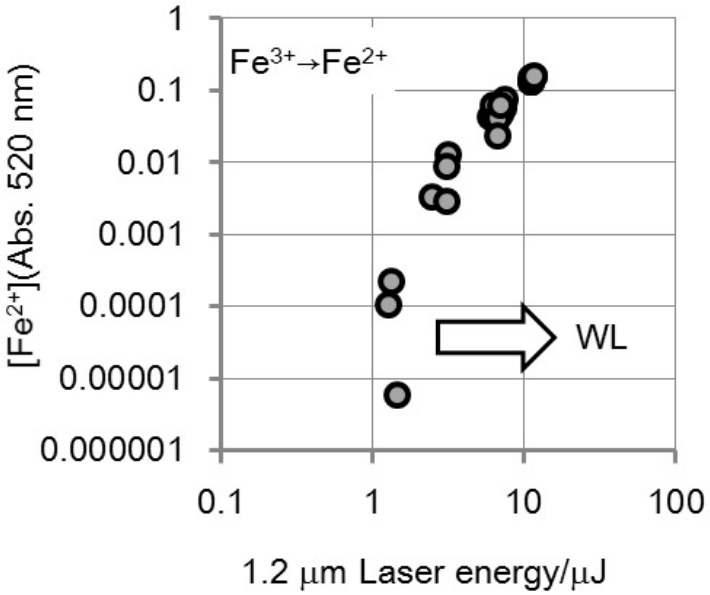

FIG. 6: $Fe^{3+} \rightarrow Fe^{2+}$ conversion on irradiation with 1190-nm, 100-fs laser pulses of 0.1 M $K_3Fe^{3+}(C_2O_4)_3$ aqueous solution. An arrow with WL is a region of energy where white-light laser visually seen.

III-3. $Ag^+ \rightarrow\rightarrow Ag_n^+$

Silver ions have been known to be reduced to Ag_n^+ by γ-ray irradiation in aqueous solutions that contain sodium polyacrylate [28]. While Ag nanoparticle formation has been reported on irradiation with femtosecond laser pulses under high laser intensities, where solvent break down occurs [28 b], the present results were obtained under weak laser intensities, where white-light laser emission was barely visible. The reducing agent is the

hydrated electron by generated γ-radiolytically. The absorption spectra of the solutions vary from rose to green or blue depending on the size of the silver clusters. Aqueous solutions containing silver ions are good systems, because we can produce solvated electrons by femtosecond laser irradiation. Figure 7 shows preliminary results for the color change of an Ag^+ ion solution by femtosecond laser pulses.

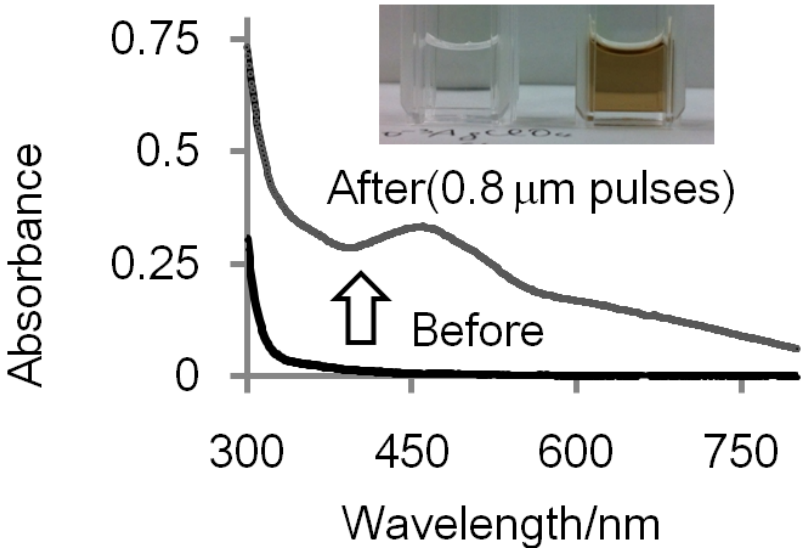

FIG. 7: A spectral change due to $Ag^+ \rightarrow\rightarrow Ag_n^+$ formation on irradiation with 800-nm femtosecond laser pulses.

Before irradiation a 0.3 ml solution in a 1-cm cell containing 6×10^{-3} M $AgClO_4$, 0.01 M PANa, and 0.13 M 2-propanol has no absorption visible region. After 100-fs, 5-μJ laser pulses at 1 kHz for 10 min, the color becomes dark brown with an absorption spectrum in the entire visible range with a broad hump around 450 nm. Interestingly, a kind of brown smoke in the cell was visible during the irradiation.

White-light laser was generated in a pulse energy range of 2–10 μJ. This observation coincides with a report in which white-light laser was studied in the presence of silver clusters with 50-fs and 800-nm laser pulses with a focal lens of 170 mm with an energy higher than 3 μJ/pulse [37]. A bright spark was seen occasionally, probably due to the cluster inducing a breakdown even at an energy of 5 μJ/pulse. We observed Ag_n^+ absorption in the energy range of weak irradiation intensities, where white-light laser is generated. The absorbance-laser intensity in logarithmic scales gave a slope of about 1.5, though the absorbance data of Ag_n^+ fluctuated widely. The absorption spectrum in Figure 7 indicates that the Ag^+ solution would require at least three photons of an 800-nm pulse to reach an excited state of this system, but the slope of the formation of Ag_n^+ vs. the laser intensity was not three but about 1.5.

IV. DISCUSSION

IV-1. Reduction with e^-_{sol} accompanied by white light laser

Three lanthanide ions (Eu^{3+}, Sm^{3+}, and Yb^{3+}) and two transition metal ions (Fe^{3+} and Ag^+) have been found to be reduced to the corresponding ions by femtosecond laser pulses accompanied by white-light laser generation. The common mechanism through these reactions, including Fe^{3+} at 1190 nm other than the case of a Fe^{3+} system by 800-nm pulse excitation, is schematically depicted in Figure 8. The interaction and related phenomena between high intensity femtosecond laser beams and liquid media have been well studied [33–35]. Briefly, an input laser beam is converged by a focusing lens and nonlinear index n_2 of the medium. An electron is injected under a high intensity laser field and the electrons play a role of defocusing due to their low index of electron. A balance between the positive and low indexes maintains a small size of the high intensity region, which is called a filament. The peak intensity in the filament is clamped and kept at approximately 10^{13} W/cm^{-2}, which is high enough to ionize solvent and generates electrons. At the same time, the laser pulse becomes steep in the filament, resulting in self-phase modulation, i.e., the input laser energy is partly converted to white-light laser. Conversion to the white-light laser proceeds before laser induced bulk breakdown (BD) in the case of femtosecond pulse excitation unless there are tight focusing conditions. The ionization causes plasma-induced defocusing, followed by multiple refocusing, which has been clearly observed [35].

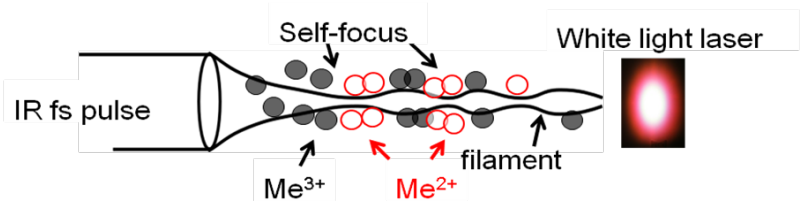

FIG. 8: Schematic diagram of the reduction of $Me^{3+} \rightarrow Me^{2+}$ and/or $Ag^+ \rightarrow Ag$ under IR femtosecond laser pulse accompanied by white-light laser.

Once an electron is ejected, the surrounding methanol/water molecules relax it to the solvated electron, e^-_{sol}, and it can then be captured by Me^{3+} and /or Ag^+. The scheme in Figure 8 is rewritten for each reduction system as in (1), (3), (4), and (5). The three lanthanide system has been described in (1). Ionization of water and relaxation to e^-_{sol} would be the first step as in (3) for the Fe^{3+} system at 1190-nm pulses and for the Ag^+ system.

$$CH_3OH/H_2O \xrightarrow{nh\nu} CH_3OH^+/H_2O^+ + e^-_{sol}, \tag{3}$$

$$[Fe^{3+}(C_2O_4)_3]^{3-} + e^-_{sol} \rightarrow [Fe^{2+}(C_2O_4)_3]^{4-}, \tag{4}$$

$$Ag^+ + e^-_{sol} \rightarrow Ag,\ Ag^+ + Ag \rightarrow Ag^+_2,\ \ldots\ldots \rightarrow Ag^+_n. \tag{5}$$

We suggest Scheme (4), in which the parent oxalate Fe^{3+} ion is reduced by e^-_{sol} following Scheme (3). The reaction with e^-_{sol} with $[Fe^{3+}(C_2O_4)_3]^{3-}$ in (4) has been discussed as a minor contribution to the photochemical one-photon reaction of $[Fe^{3+}(C_2O_4)_3]^{3-}$ with a high rate constant of 1.2×10^{10} $M^{-1}s^{-1}$ [24]; in other words, (4) is an efficient reaction if e^-_{sol} is present. It is notable that at least five 800-nm photons are required to be absorbed to ionize the media on the based on the band gap in methanol of 6.2 eV methanol [35]and in water of the I_p of 6.5 eV [38].

After a solvent molecule is ionized, a few events follow. We estimate that about a half of the initially ejected electrons could react with the metal ions. Immediately after the ionization, the electron will be solvated to less than 1 ps to form e^-_{sol} [36]. The next event would be geminate recombination between the parent cation and e^-_{sol}. Photoionization studies in neat water at room temperature have been performed in a picoseconds timescale. After the electron has been solvated, the geminate recombination occurs in roughly 60 ps with 40-50% of the electrons, in other words, 50–60% of e^-_{sol} escape from the initial pair [40]. The escaped electron has a high possibility of reaction with metal ions. The reaction rate constants between metal ions and e^-_{sol} have been accumulated in the field of radiation chemistry [12]and are 1–5 $\times 10^{10}$ $M^{-1}s^{-1}$ for the present metal ions. The reaction time is 0.2–1 ns for the case of 0.1 M metal ion concentration. Major competing reactions would be $e^-_{sol} + O_2 \rightarrow O_2^-$ with 1.9×10^{10} $M^{-1}s^{-1}$ [12], which is in 200 ns, and $e^-_{sol} + e^-_{sol}$ quenching with a rate constant of 1.1×10^{10} $M^{-1}s^{-1}$, which will be in 100 ns time scale. These time scales are estimated assuming $[e^-_{sol}] \sim 9 \times 10^{-4}$ M based on 55% of initially generated electron of 10^{18} cm^{-3} in filaments [34] and $[O_2] \sim 2.8 \times 10^{-4}$ M in an air saturated solution. As a conclusion, the major reaction would occur between metal ions and e^-_{sol}, and a half of the initially ejected electrons can be trapped by metal ions for the case of 0.1 M of a metal ion solution. To experimentally determine the trapping efficiency, we need information on the electrons ejected/unit filament, and the number of filaments, although we roughly estimated the efficiency of 0.2 for the case of Eu^{3+} reduction [4].

IV-2. Two photon absorption followed by reduction

For the Fe^{3+} system at 800-nm pulses, two-photon excitation to the CT state followed by the normal photochemical reaction of Scheme (2) proceeds. Formation of Fe^{2+} was clearly observed with keeping the slope of two even in an energy range lower than the threshold laser intensity of white laser emission as in Figure 5.

At 800 nm, the conversion efficiencies of the reduced metal ion numbers divided by the input photon numbers were evaluated to be 0.052 for Fe^{2+} formation from Figure 5. The input laser energy was measured to be absorbed by Fe^{3+} solution by 10 % more than that by pure water. The single-photon photochemistry of Fe^{3+} complex has the yields of 1.13 (392 nm)-1.14 (405 nm) [20]. The observed conversion efficiency of 0.052 is close to the expectation; 0.1(absorption of 800-nm laser pulse) ×1.13 (yield of the excited CT state at 405 nm)/2(two-photon) = 0.057. It is very reasonable for the two photon chemistry. The two-photon coefficient was reported as 1.5×10^{-50} cm^4 s/photon at 694.3 nm [25]. This value is equivalent to the molar extinction coefficient of 150 $M^{-1}cm^{-1}$ at 10^{13} Wcm^{-2}. The absorbance at 10 μJ of the 800-nm pulse was 0.05; therefore, the two-photon coefficient at

800 would be on the order of 0.05×10^{-50} cm^4 s/photon, if the filament length was 0.1 cm.

The CT level of $[Fe^{3+}(C_2O_4)_3]^{3-}$ can be reached by three photon absorption of 1190-nm pulses and the CT state Yb^{3+} by three-photon absorption of 800-nm pulses; however, the results in Figures 3 and 6 cannot be explained in terms of the slopes of three. The order for the n th-multiphoton absorption and reactions sometimes go into behind the scene, in the intensity region where self-focusing of the laser beam occurs [26, 27]. In those organic molecules, the multiphoton absorption was clearly observed under the threshold of the white-light laser [26, 27]. The reduction due to two-photon absorption was observed well under the threshold of the white-light laser for the Fe^{3+} system by 800-nm pulse excitation.

IV-3. To Fe^{2+} at 1190 nm with an efficiency of 10^{-3}

The efficiencies of the reduced metal ion numbers divided by the input photon numbers can be evaluated to be 0.001 for Yb^{2+} at 800 and 970 nm from Figures 2 and 3, and 0.0016 for Fe^{2+} at 1190 nm from Figure 6, in all cases at 10 μJ/pulse. The same order of the efficiencies for the two different chemical systems is a good indication to hold the same reduction mechanism. The absorbance of 0.05 at 367 nm for Yb^{2+} in Figures 2 and 3 was obtained by 1.8×10^5 shots irradiation of 10 μJ/pulse. Using the molar extinction coefficient of 500 $M^{-1}cm^{-1}$ and the excitation volume of 0.04 cm^3, the produced Yb^{2+} was evaluated to be 1.0×10^{-8} mol and the input photons were 1.2×10^{-5} E (Einstein = mol photon). Therefore the conversion efficiency was on the order of 10^{-3}. There are two steps for the reduction. The first step is the formation of e^-_{sol} and the second one is the trapping reaction of e^-_{sol} by the metal 3+ ions. To reach the coincidence the efficiencies, the rate constants between the metal 3+ ions and e^-_{sol} should be similar. In fact, they are on the same order; 1.5×10^{10} $M^{-1}s^{-1}$ for the oxalate Fe^{3+} system [24] and 4.3×10^{10} $M^{-1}s^{-1}$ for Yb^{3+} aqueous solution [12].

If the mechanism of three-photon absorption followed by reduction worked for 1190-nm excitation, the efficiency at 1190 nm should be reduced to 10^{-3} times of that of the two-photon absorption, according to the absorption cross section ratio between three photon ($\sigma^{(3)}I^2$) versus two-photon one ($\sigma^{(2)}I$), where the laser intensity I is 10^{13} W/cm^2 (3.8×10^{31} photons $cm^{-2}s^{-1}$ at 800 nm and 5.7×10^{31} photons $cm^{-2}s^{-1}$ at 1190 nm, under 3 μJ in 100 fs and 20 μm diameter). We adopt $\sigma^{(3)}/\sigma^{(2)} \approx 10^{-35}$ photons^{-1}cm^{2}s according to a review about n-photon absorption on atoms [39]; therefore,

$$\text{Crosssectionratio} = \frac{\sigma^{(3)}I^2(1190\,\text{nm})}{\sigma^{(2)}I(800\,\text{nm})} \approx 1 \times 10^{-3}. \tag{6}$$

The observed efficiency ratio at 1190 nm vs. that at 800 nm was $0.0017/0.052 \approx 0.03$, and is 30 times larger than that of the expected value of 10^{-3} in Eq. 6. The high conversion to Fe^{2+} at 1190 nm can be another reason that suggests the reduction mechanism is not the three-photon absorption process but formation of e^-_{sol} followed by reduction. Although we may not directly apply a parameter in atoms to the Fe^{3+} complex, it is not unreasonable to indicate the low reduction efficiency by three-photon absorption mechanism.

V. CONCLUSIONS

The following points from the Introduction have been made clear. i) Yb^{3+} system has been realized to show a reaction of $Ln^{3+} + e^-_{sol} \rightarrow Ln^{2+}$, which is similar with the Eu and Sm systems. Now three lanthanide ions, which have fast reaction rate constants of e^-_{sol} in the literature [12–14] and have low redox potentials [41], show the same behavior. ii) We have succeeded in extending two transition metals of Fe^{3+} at 1190-nm excitation, and Ag^+ at 800 nm. Whenever white-light laser is emitted, the reactions have been detected to Fe^{2+} and Ag^+_n. iii) An Fe^{3+} system by 800-nm excitation, Fe^{2+} was detected even lower than the white laser threshold and was explained in terms of two-photon reaction. iv) Now we know that three lanthanide ions Ln^{3+} (Ln = Eu, Sm, Yb) and two transition metals (Fe^{3+} and Ag^+) were found to be reduced to the corresponding Ln^{2+}, Fe^{2+}, and Ag_n by e^-_{sol} generated by femtosecond laser pulses. These reactions are along the same lines as those in radiation chemistry, as we have already suggested when we observed the $Eu^{3+} \rightarrow Eu^{2+}$ reaction as the first example [4]. These reactions could be very general and the accumulated results in the radiation chemistry can be used as reliable references. We need to study more in detail, because there must be some differences in chemistry among femtosecond laser with white laser, laser induced break down, and γ-ray radiation. Recently, femtosecond filamentation has been applied to cancer therapy [7]. Studies on various chemical reactions by femtosecond filamentation would be helpful to understand the chemical reactions in cancer therapy.

Acknowledgements

This work was financially supported in part by a Grant-in-Aid (No. 23550030) from the Ministry of Education, Culture, Sports, Science, and Technology of Japan to N.N.

References

[1] S. L. Chin *et al.*, Laser Physics **22**, 1 (2012).
[2] P. Rohwetter *et al.*, Nature Photonics **4**, 451 (2010).
[3] T. Fuji and T. Suzuki, Opt. Lett. **32**, 3330 (2007).
[4] D. Nishida, M. Kusaba, T. Yatsuhashi, and N. Nakashima, Chem. Phys. Lett. **465**, 238 (2008).
[5] D. Nishida, E. Yamade, M. Kusaba, T. Yatsuhashi, and N. Nakashima, J. Phys. Chem. A **114**, 5648 (2010).
[6] T. Yatsuhashi, N. Uchida, and K. Nishikawa, Chem. Lett. **41**, 722 (2012).
[7] R. Meesat *et al.*, Proc Natl Acad Sci USA **110**, 3651 (2013).
[8] J. Qiu, K. Kojima, K. Miura, T. Mitsuyu, and K. Hirao, Opt. Lett. **11**, 786 (1999).
[9] H. You and M. Nogami, J. Phys. Chem. B **109**, 13980 (2005).
[10] A. Ishida and S. Takamuku, Chem. Lett. **1988**, 1497 (1988).
[11] D. L. Selin, N. P. Tarasova, A. V. Malkov, and G. A. Poskrebyshev, React. Kinet. Catal. Lett. **39**, 273 (1989).
[12] G. V. Buxton, C. L. Greenstock, W. P. Helman, and A. B. Ross, J. Phys. Chem. Ref. Data **17**, 513 (1988).

[13] E. J. Hart and M. Anbar, *in The Hydrated Electron* (Wiley-Interscience, New York, 1970).
[14] W. T. Carnall, *in Handbook on the Physics and Chemistry of Rare Earths*, eds. K. A. Gschneidner, Jr. and L. Eyring (North Holland Publ. Co., Amsterdam, 1979, Vol. 3), Chapter 24, pp 172-208.
[15] M. Kusaba, N. Nakashima, Y. Izawa, W. Kawamura, and C. Yamanaka, Chem. Phys. Lett. **197**, 136 (1992).
[16] M. Kusaba, Y. Tsunawaki, and N. Nakashima, J. Photochem. Photobiol. A: Chem. **104**, 35 (1997).
[17] N. Nakashima, K. Yamanaka, and T. Yatsuhashi, J. Phys. Chem. A. **117**, 8352 (2013).
[18] M. Kusaba, N. Nakashima, Y. Izawa, C. Yamanaka, and W. Kawamura, Chem. Phys. Lett. **221**, 407 (1994).
[19] C. A. Parker, Roc. R. Soc. London, Ser. A, **220**, 104 (1953).
[20] S. L. Murov, *Handbook of Photochemistry* (Marcel Dekker. Inc. New York, 1973).
[21] I. P. Pozdnyakov, O. V. Kel, V. F. Plyusnin, V. P. Grivin, and N. M. Bazhin, J. Phys. Chem. A **112**, 8316 (2008).
[22] J. Chen, A. S. Dvornikov, and P. M. Rentzepis, J. Phys. Chem. A **113**, 8818 (2009).
[23] I. P. Pozdnyakov, O. V. Kel, V. F. Plyusnin, V. P. Grivin, and N. M. Bazhin, J. Phys. Chem. A **113**, 8820 (2009).
[24] J. Chen, H. Zhang, I. V. Tomov, and P. M. Rentzepis, Inorg. Chem. **47**, 2024 (2008).
[25] H. Zipin and S. Speiser, Chem. Phys. Lett. **31**, 115 (1975).
[26] T. Yatsuhashi, S. Ichikawa, Y. Shigematsu, and N. Nakashima, J. Am. Chem. Soc. **130**, 15264 (2008).
[27] T. Yatsuhashi, Y. Nakahagi, H. Okamoto, and N. Nakashima, J. Phys. Chem. A **114**, 10475 (2010).
[28] a) B. G. Ershov and A. Henglein, J. Phys. Chem. B **102**, 10663 (1998); b) T. Nakamura, H. Magara, Y. Herbani, and S. Sato, Appl. Phys. A **104**, 1021 (2011).
[29] T. Yatsuhashi and N. Nakashima, J. Phys. Chem. A **109**, 9414 (2005).
[30] K. Yamanaka and T. Morikawa, J. Phys. Chem. C **116**, 1286 (2012).
[31] B. Keller, K. Bukietyńska, and B. Jeżowska-Trzebiatowska, Bull. Acad. Pol. Sci. Ser. Sci. Chim. **24**, 763 (1976).
[32] T. Kimura, R. Nagaishi, Y. Kato, and Z. Yoshida, Radiochim. Acta. **89**, 125 (2001).
[33] V. P. Kandidov *et al.*, Appl. Phys. B **77**, 149 (2003).
[34] S. L. Chin *et al.*, Can. J. Phys. **83**, 863 (2005).
[35] W. Liu, S. L. Chin, O. G. Kosareva, I. S. Golubtsov, and V. P. Kandidov, Opt. Commun. **225**, 193 (2003).
[36] M. Mizuno, S. Yamaguchi, and T. Tahara, J. Phys. Chem. A **109**, 5257 (2005).
[37] C. Wang, Y. Fu, Z. Zhou, Y. Cheng, and Z. Xu, Appl. Phys. Lett. **90**, 181119 (2007).
[38] D. N. Nikogosyan, A. A. Oraevsky, and V. I. Rupasov, Chem. Phys. **77**, 131 (1983).
[39] M. V. Ammosov, N. B. Delone, M. Y. Ivanov, I. I. Bondar, and A. V. Masalov, Adv. Atomic. Molec. Phys. **29**, 33 (1991).
[40] H. Lu, F. H. Long, R. M. Bowman, and K. B. Eisenthal, J. Phys. Chem. **93**, 27 (1989).
[41] L. R. Morss, Chem. Rev. **76**, 827 (1976).